ESCA INVESTIGATIONS ON PLASTIC-BONDED NICKEL OXIDE ELECTRODES

J. JINDRA, I. KREJČÍ and J. MRHA

J. Heyrovsky Institute of Physical Chemistry and Electrochemistry, Czechoslovak Academy of Sciences, 10200 Prague 10 (Czechoslovakia)

B. FOLKESSON, L. Y. JOHANSSON and R. LARSSON

Inorganic Chemistry 1, Chemical Center, University of Lund, P. O. Box 740, 22007 Lund 7 (Sweden)

(Received December 16, 1983; in revised form March 1, 1984)

Summary

Electrode samples, prepared by a rolling technique from an active mass, graphite and Teflon mixture, were characterized by ESCA (X-ray photoelectron spectroscopy) before operation, after a short electrochemical formation, and after a certain number of charge–discharge cycles. The spectra of F_{1s}, C_{1s}, O_{1s} and $Ni_{2p_{3/2}}$ were measured in detail.

A splitting of the F and C signals (from Teflon) in the Teflon–graphite mixture was interpreted as indicating different qualities of contacts between the Teflon and graphite particles. The change in character of this contact resulting from cycling of the electrode was followed and was considered to be the cause of the change of the electric resistance in the electrode.

From the decrease of the intensity of the Ni signal one can conclude that part of the $Ni(OH)_2/NiO(OH)$ system withdraws from the surface of the graphite particle structure during prolonged operation of the electrode. This effect is caused by a partial crystallization of the hydrated Ni(II)–Ni(III) oxide system which, in its turn, causes discontinuities in the hydrogel to appear, reflected by an increase in the F_{1s} signal intensity.

Introduction

In $Ni(OH)_2/NiO(OH)$ positive electrodes of alkaline storage batteries one often observes a distinct decrease of the electrode capacity, especially when high discharge rates are used.

In batteries with sintered electrodes this effect is not so distinct but it is very pronounced in pocket-type electrodes and to some extent in plastic bonded nickel oxide (PB-Ni) electrodes. These observations led, *inter alia*, to

0378-7753/84/$3.00

the general conclusion that the decrease of electrode capacity is largely controlled by ohmic conditions in the electrode [1, 2]. PB-Ni electrodes have been developed to obtain systems of high energy content per unit mass in comparison with the conventional pocket electrodes [3]. The former kind of electrodes are also better suited for mass-production. The main principle of these PB-Ni electrodes is that of the incorporation of particles of a commercially available active mass (mainly $Ni(OH)_2$ and graphite) into a conductive, elastic network based on a graphite–Teflon mixture.

Some findings (*e.g.*, the colouring of the electrolyte after cycling of PB-Ni electrodes) suggest that both the graphite particles that are part of the above-mentioned network and those that belong to the active mass are detrimentally affected. In order to improve the understanding of the decrease of capacity and the shift of the discharge curve towards more negative potentials when heavy loads are used, we have undertaken an ESCA investigation on some electrode samples before and after the electrochemical process. As ESCA is a surface-sensitive technique [4], changes in the outermost layers of the material investigated are detected.

As the physical properties of the surface layers of an electrode are more important for the electrochemical performance than those of the bulk material, one might hope that valuable information will be secured in this way. This information could be used to improve the construction of the electrodes.

Experimental

Electrochemistry

The PB-Ni electrodes (4 × 7.5 cm) were prepared by a rolling technique [5] from electrode mixtures containing 85% commercial active mass, 7.5% PTFE and 7.5% graphite onto net-type, nickel-plated collectors of various wire diameters and mesh size. The testing procedure has been described previously [6].

The electrodes were first formed for 3 cycles using 15 h charging at 0.2 A and discharging at 0.3 A to a cut-off potential of 0.0 V *vs.* an Hg/HgO reference electrode in the same solution (KOH, 1.2 g cm^{-3}) separated from the electrode by a Haber–Luggin capillary. Thereafter the electrodes were subjected to long term testing at a high discharge rate (6 A per electrode, *i.e.*, 100 mA cm^{-2}) to a cut-off potential of −0.5 V. The detailed electrochemical treatment is described in Table 1, presenting the electrode samples actually used for ESCA measurements.

The samples of graphite CR-12 were pressed into circular tablets, wrapped afterwards in a fine nickel gauze, and again pressed at a high pressure.

TABLE 1

Description of the samples investigated

Sample no	Composition	Electrochemical treatment
1	graphite CR-12	none
2	graphite + Teflon	none
3	graphite	cathodic (H_2 evolution)
4	graphite	anodic (O_2 evolution)
5	graphite	4 cycles: charging 1.5 A (1 h) discharging 1 A (1 h)
6	85% active mass 7.5% graphite 7.5% Teflon	none
7	see sample 6	three formation cycles
8	see sample 6	four high-rate dischargings (6 A)
9a	see sample 6	200 high-rate dischargings (6 A)
9b		charged once more
10	Teflon	

ESCA

The ESCA measurements were carried out with an AEI ES 200 instrument. The samples scraped off the electrode active layers were pressed onto a fine-meshed copper grid.

In the case of pure graphite (sample 1) the substance was pressed into a lead foil in order to achieve a good adherence.

The surface exposed for ESCA characterisation is thus a composite one, containing both formerly internal and formerly external surfaces of the working electrode. Both of these types of surfaces, and especially the second one, will reflect any change in the concentration gradients within the nickel hydroxide gel system.

An overall spectrum was first recorded for each sample and thereafter the special parts of interest, *i.e.*, C_{1s}, F_{1s}, O_{1s} and Ni_{2p}. The binding energies were calculated from the formula

$$E_b = 1484.6 - E_{kin} \quad (1)$$

where the term 1484.6 (eV) contains the correction for the work function. The kinetic energy, E_{kin}, is the experimentally determined quantity.

Results and discussion

Electrochemistry

The electrochemical performance of a typical PB-Ni electrode (No. 6 of Table 1) was followed up to 200 charge–discharge cycles. During cycling the following currents were used:

1 - 100 cycles: 2 h charging at 1.2 A and discharging at 6 A;
101 - 122 cycles: 2 h charging at 2.0 A and discharging at 6 A;
123 - 200 cycles: 1 h charging at 3.0 A and discharging at 6 A.

The results of such electrochemical treatment (Sample No. 9 of Table 1) are given in Figs. 1 - 3. One can observe that there is a remarkable shift of discharge characteristics at 100 mA cm^{-2} current load towards more negative potentials (Fig. 1) and, consequently, the time needed to reach the potential 0 V is shorter (Fig. 2) when more than 100 cycles have been run.

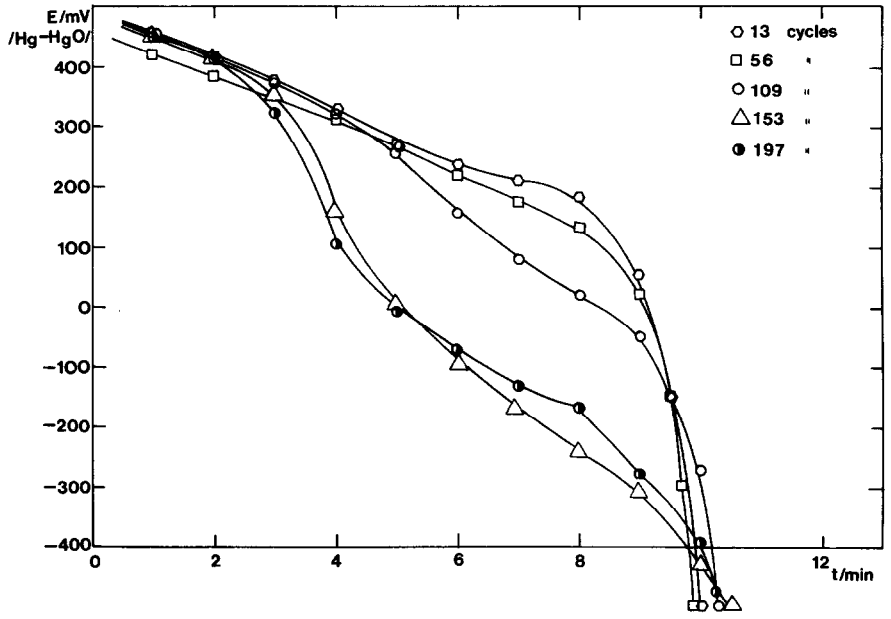

Fig. 1. Discharge curve for a heavy discharge, 6 A per electrode, *i.e.*, 100 mA cm^{-2}, for sample 6.

Contrary to what is the case for the heavy discharge load, the performance of the same electrode at low discharge rates is generally not markedly influenced by the cycling (Fig. 3). These results can be interpreted as being caused by an increase in contact resistivity between electrochemically active particles and the conductive graphite particles. All other electrochemical measurements were made only for a more complete elucidation of the capacity decay of PB-Ni electrodes.

ESCA

The results of ESCA measurements are best presented graphically. Detailed information is given in Table 2. In Fig. 4 we present the spectra of pure graphite, pure Teflon, and the mixture of both materials that was used for the preparation of the PB-Ni electrodes. In this and the following Figures the energy scale is that of the kinetic energy actually measured. In Figs. 4 - 7 we have given the proper binding energies of the electrons at their respective

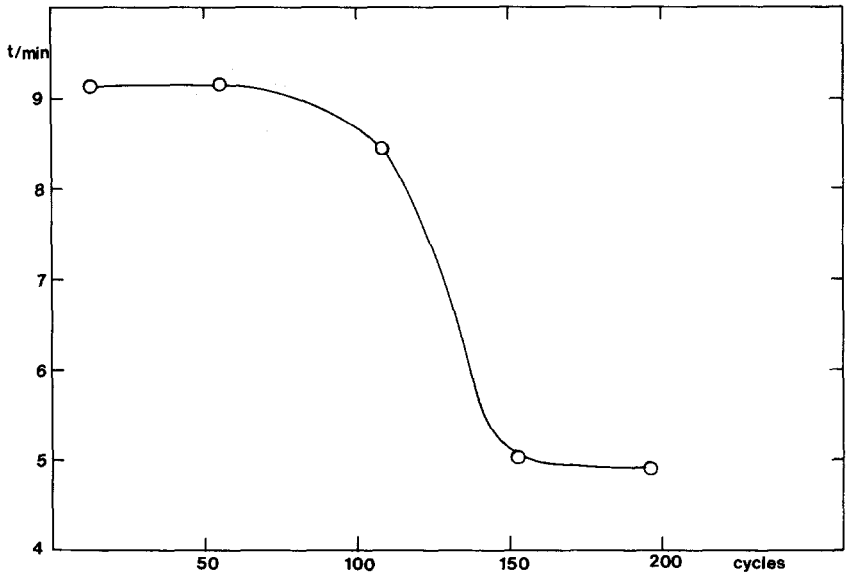

Fig. 2. Presentation of the time necessary to reach the electrode potential of 0 mV relative to an Hg/HgO electrode for the cycling tests of Fig. 1.

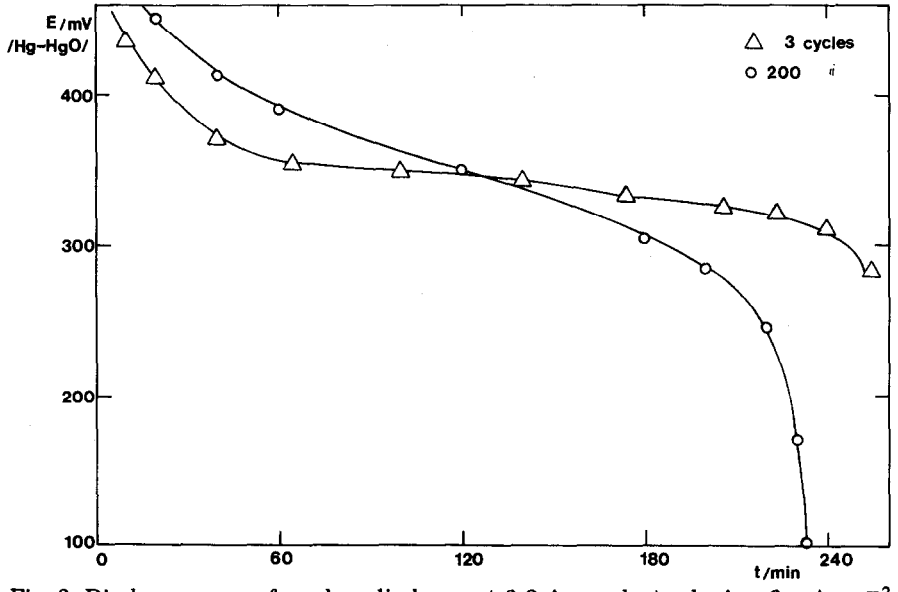

Fig. 3. Discharge curves for a low discharge at 0.2 A per electrode, *i.e.*, 3 mA cm^{-2}.

peak maxima. The binding energy of C_{1s} in graphite was used as a reference value, $E_b(C_{1s})$ = 284.3 eV [7]. This peak was overwhelmingly the most intense of the carbon spectrum.

TABLE 2

Experimental binding energies (eV)

Sample (*cf.* Table 1)	F_{1s}		O_{1s}			C_{1s}		$Ni_{2p_{3/2}}$	
2	691.3	689.1				294.5 292.1	284.3		
6	691.6	688.8	534.3	531.6			284.3	858.6	855
7	691.0	689.0	532.4	530.6			284.3		854.5
8	690.8	689.0	532.2	530.0	528.8		284.3		854.3
9a	691.0	689.0	532.1	530.1			284.3		854.4
9b	691.1	689.0	(534) 529.9	532.2 (528)			284.3	858	854.3

All values are referred to the binding energy of carbon in graphite = 284.3 eV. The intensities are not given here but are indicated in Figs. 5 - 7. The composite peaks have been resolved by a subjective fit of peak positions and intensities.

(i) Graphite

As a first result we can report that there was no significant difference between the C_{1s} spectra of samples 1, 3, 4, and 5 of Table 1. This means that the three different short term electrochemical treatments (see Table 1; samples 3 - 5) are without considerable effect on the carbon surface. Additionally, the possible surface oxidation might be localized onto the outer surface of the tablets. In order to prepare a sample for ESCA measurements the original tablets had to be mechanically disintegrated and any surface oxides possibly formed might be "diluted" or even hidden by non-oxidized graphite particles from the bulk of the tablet.

In the course of our further work we found another cause of the decay of electrochemical activity of the PB-Ni electrodes other than that of graphite deterioration. Therefore we did not follow up the problem of graphite oxidation.

(ii) Graphite + Teflon

As a second observation (see Fig. 4) one notes a remarkable two-peak structure of both the C_{1s} and the F_{1s} spectra of Teflon in the graphite–Teflon mixture. This is probably caused by differential charging of the Teflon particles [8]. One group of particles, corresponding to the peaks with high kinetic energy (E_b = 689.0 eV), is in "good" electric contact with the graphite. The other group of particles, corresponding to low kinetic energy (E_b = 691 eV), has attained a certain extra positive charge, *i.e.*, the particles are not in good contact with the graphite. This charging effect is well known as a scourge of ESCA work on insulating materials [4]. The similar magnitude of the peak shifts in both the F_{1s} and the C_{1s} spectra (*cf.* sample 2, Table 2) is in favour of this assignment. The most probable cause for the observed difference in

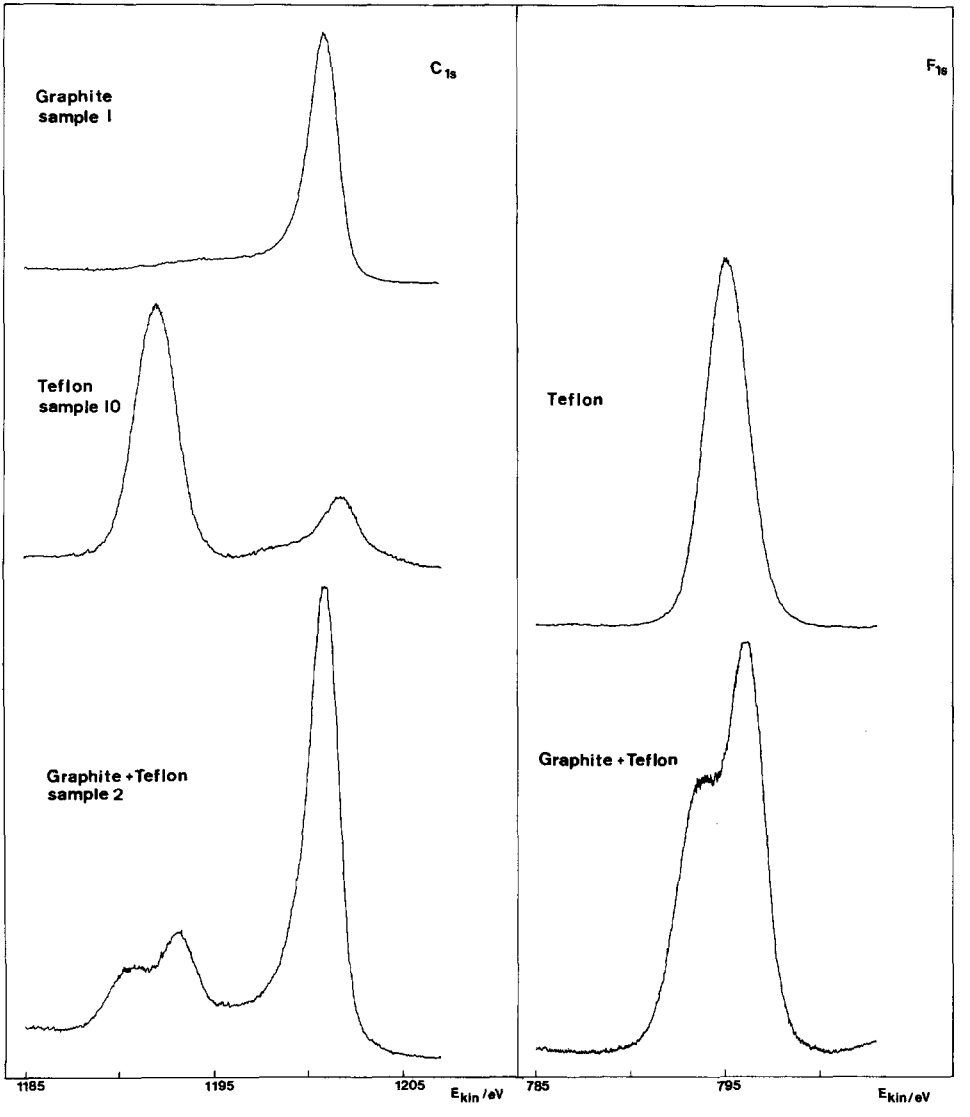

Fig. 4. Spectra of C_{1s} and F_{1s} core electrons from graphite, Teflon, and the mechanical mixture of graphite and Teflon.

charging is that the Teflon particle can be located in one of two different situations: Teflon–graphite contact and Teflon–Teflon contact, respectively.

(iii) The freshly fabricated electrode

We now discuss the spectral changes happening in the sequence when the electrodes are fabricated, when they are electrochemically formed, and when they are subjected to repeated cycles of heavy discharging/charging. In Figs. 5 - 7 we present the relevant graphs for samples 6, 7, 8, 9a and 9b, giving spectra of F_{1s}, O_{1s} and Ni_{2p}, respectively.

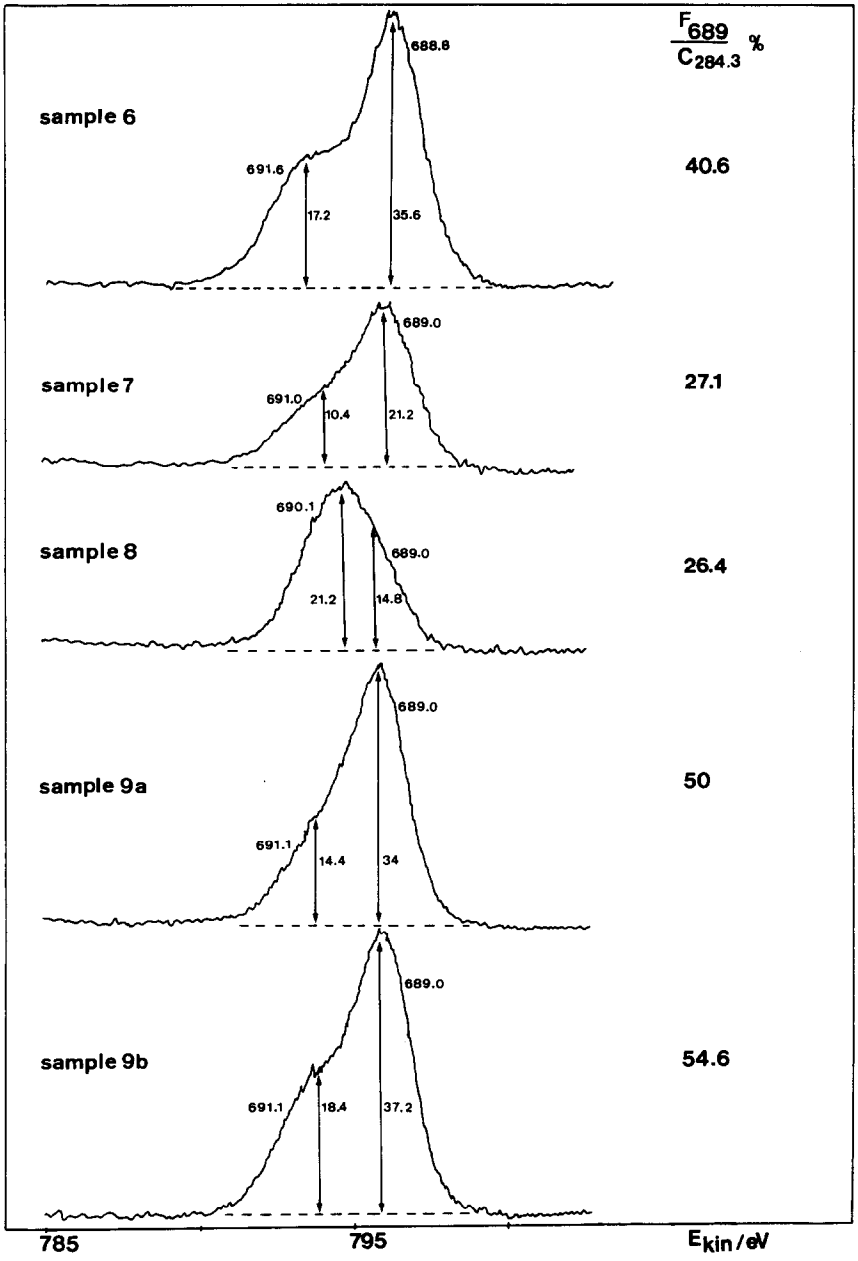

Fig. 5. Spectra of F_{1s} core electrons for samples 6 - 9, treated as given in Table 1. The intensities are given in 10^2 cps. The varying charge of the samples affects the position of the spectra on the abscissa axis. The binding energies are obtained by using the calibration value of graphite, $E_b(C_{1s})$ = 284.3 eV. The numbers on the right hand side of the Figure indicate relative intensities, fluorine (at the indicated E_b) to carbon (graphite).

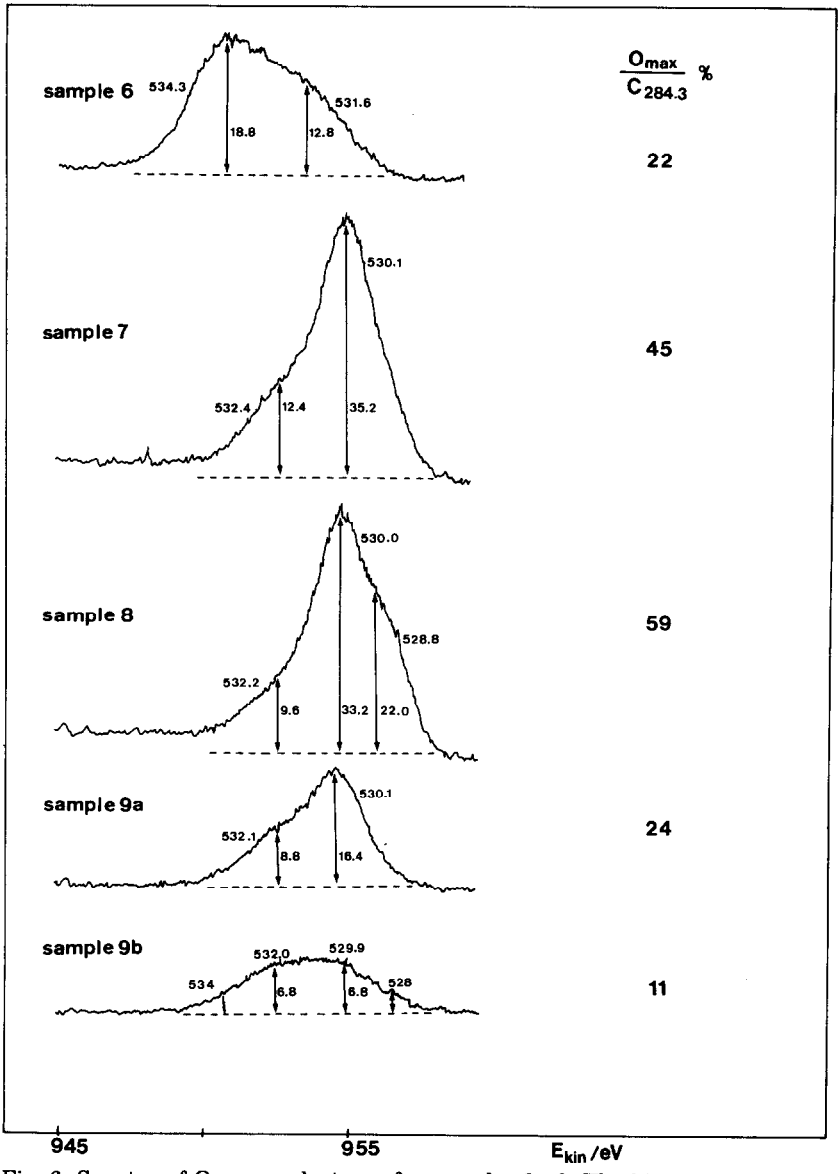

Fig. 6. Spectra of O_{1s} core electrons for samples 6 - 9. The binding energy values refer to the positions marked by arrows. Other conditions and notations as in Fig. 5.

The first observation for comment is the difference between the F_{1s} spectra of sample 6 (Fig. 5) and sample 2 (Fig. 4). The splitting that was clearly observed before is now not very well resolved. This means that there is a larger range of potentials that the Teflon particles can acquire. Most probably, the presence of particles of the electrochemically active, semiconducting nickel hydroxide system causes a set of new possibilities for contact between Teflon and graphite. Indeed, most of the nickel hydroxide particles appear

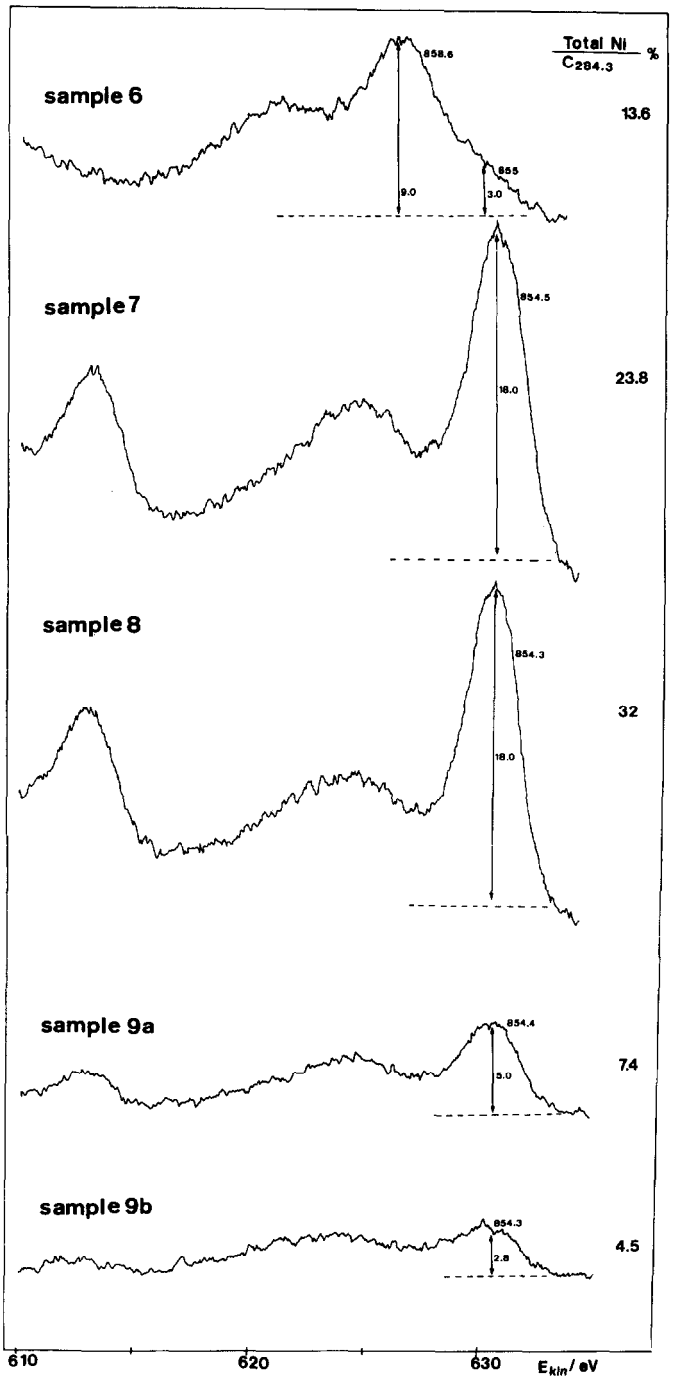

Fig. 7. Spectra of Ni_{2p} core electrons for samples 6 - 9. The intensity ratio Ni/C is given to the right with "Total Ni" meaning the estimated sum of the main peaks of Ni of various kinetic energies caused by charging from the X-ray irradiation.

to be screened from the main graphite material by Teflon. This follows from the observation (Figs. 6 and 7, sample 6) of strong, low kinetic energy peaks of O_{1s} and $Ni_{2p_{3/2}}$.

(iv) The electrode after electrochemical formation

Turning our attention now to the spectra of sample 7, *i.e.*, after electrochemical formation, one observes above all that the intensity of F_{1s} relative to C_{1s} decreases (see Figs. 5 - 7), on the other hand, the intensities of O_{1s} and $Ni_{2p_{3/2}}$ increase.

One also observes that the nickel spectrum indicates the presence of only one type of nickel. This is interpreted to mean that the presence of the electrolyte (KOH) causes a continuous nickel hydroxide gel — consisting of both Ni(II) and Ni(III) — to develop from which one cannot distinguish any individual particles. Moreover, one observes that the intensity increases of O_{1s}/C_{1s} and of Ni_{2p}/C_{1s} have about the same relative magnitude. This latter observation must mean that the oxygen signal mostly originates from the nickel hydroxide gel.

We imagine the situation existing after this first electrochemical treatment to be somewhat similar to that depicted in Fig. 9(a). The Teflon particles have to some extent lost contact with the graphite particles and are more or less covered by the continuous gel. The graphite particles are in good contact with each other and with the nickel hydroxide gel.

(v) The first few cycles

On repeated cycling (4 times, sample 8), this trend is more pronounced. One observes, for example, that the F_{1s} signal now consists of a larger proportion from the highly charged particles — *i.e.*, those that are not graphite supported.

Another effect found after these four cycles is the appearance of a new oxygen signal (Fig. 6) at the low binding energy side (1.2 eV lower). This new peak is most probably related to an increased concentration of KOH in the gel at this stage.

This interpretation is further strengthened by the observation from the overall spectra, not reproduced here, that the K_{2p} signal is much more intense for sample 8 than it is for sample 7.

(vi) Effects of prolonged cycling

The most striking difference between the spectra of samples 9 and 8 is that the O_{1s} and Ni_{2p} intensities (relative to carbon) strongly decrease in magnitude. Indeed, it appears that the decrease for oxygen and that for nickel are interrelated, see Fig. 8. On the other hand, the F_{1s}/C_{1s} ratio is strongly increased. The intensity pattern (Fig. 8) for F_{1s} is the inverse of that of Ni and O.

Another effect worth commenting on is that the band contour of $Ni_{2p_{3/2}}$ on the low kinetic energy side of the main peak is much more complex than it was for the pure satellite structure of Fig. 7, sample 7.

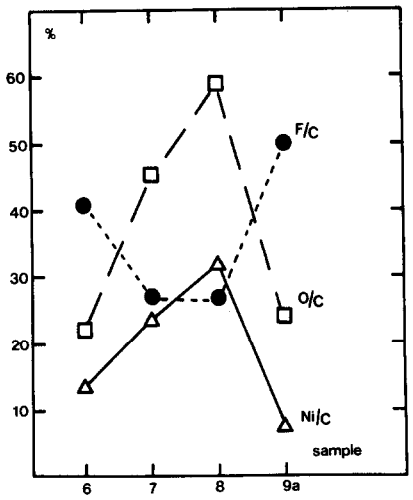

Fig. 8. Representation of intensity changes found for F_{1s}, O_{1s} and $Ni_{2p_{3/2}}$ relative to the intensity of the main C_{1s} peak for the various samples mentioned in the text.

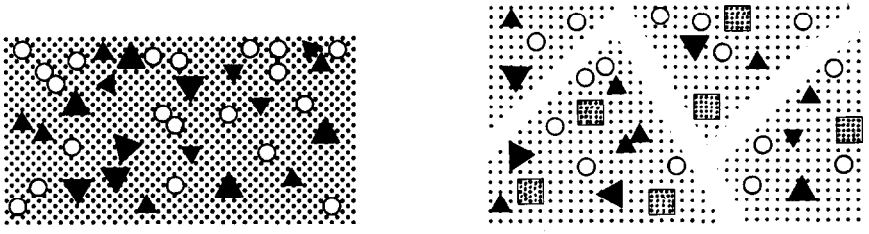

(a) (b)

Fig. 9. (a) Schematic model of the electrode after the first formation cycle. The continuous Ni(II, III) hydroxide gel is represented by the dotted background. ▲, graphite particles; ○, Teflon particles. If the representation is looked upon as the depth profile of a part of the electrode material, the depth of observation of ESCA is only a fringe part.
(b) The corresponding model of the electrode after a long term cycling. The gel is now cracked into major areas ("islands") and is characterized by a lower density. In addition, crystals have begun to form, depicted by ▣.

This latter observation might indicate a reversal to the situation of the electrochemically untreated system (Fig. 7, sample 6) where part of the nickel hydroxide was in non-conducting contact with carbon at the surface.

The decrease in Ni intensity could mean that the originally continuous gel, created in the course of the first few cycles, is partly destroyed by the many charge and discharge cycles. This destruction of the gel might be caused partly by crystallization (to large particles) and partly by cracking of the originally continuous gel following the changes (swelling on discharge; shrinking on charging) of the active layer of the PB-Ni electrode during the accelerated long term cycling. This results in the creation of small "islands" of gel that are in different electrical contact with each other and with the current collector. At heavy discharge rates (6 A) these islands are partici-

pating in the electrochemical process at different voltage levels (Fig. 1). At low discharge rates, however, this ohmic control is not dominating and almost all islands can participate in the discharge process at the same voltage level. This level, furthermore, is the same as that observed for the first cycles of the electrode (Fig. 3).

The creation of crystallites would deplete the surface of nickel and oxygen relative to the graphite network, thus decreasing the intensity of the ESCA spectra (Fig. 8). The disintegration of the originally continuous gel creates improved possibilities for the Teflon particles to appear close to the surface (total F_{1s} intensity increases). Such spectrum trends are actually found. Indeed, it is interesting to point out that for sample 9b (the electrode is recharged), one finds spectra where the trend described above is even more clearly seen. This observation is probably related to the increased shrinkage of the gel structure as a result of the appearance of the highly charged positive ion (Ni^{3+}), with its smaller radius (compared with the Ni^{2+} ion) and strong attraction for the OH^- ions and water dipoles in the immediate vicinity. In this case, of course, the Ni spectrum is also complicated by the presence of Ni(III).

Conclusions

From our investigations the following conclusions can be drawn:

(i) ESCA measurements (C_{1s} spectra) prove that surface oxidation of graphite particles might not be the main cause of the clearly observable decrease of the capacity of plastic-bonded $Ni(OH)_2/NiO(OH)$ electrodes during accelerated long-term cycling.

(ii) ESCA spectra of electrodes without any electrochemical treatment show that the particles of the electrochemically active nickel hydroxide appear to be screened by Teflon from the main graphite material.

(iii) The first, short-term electrochemical treatment causes the creation of a continuous nickel hydroxide gel which is manifested in ESCA spectra by a distinct intensity increase for both O_{1s}/C_{1s} and Ni_{2p}/C_{1s}.

(iv) The long term accelerated cycling causes a distinct decrease of the capacity of the electrodes. This decrease is accompanied by a strong decrease in magnitude of O_{1s} and Ni_{2p} intensities (relative to carbon). The close connection between changes of intensities for oxygen and nickel shows that the Ni and O signals are related to the nickel hydroxide gel.

(v) The main reason for the distinct power decrease might be interpreted in terms of the disintegration of the originally continuous nickel hydroxide gel into small "islands" having different ohmic conditions when involved in the discharge process at heavy current drains.

(vi) The reason for the gel disintegration is the drastic volume changes taking place during electrode cycling. The ohmic quality between the disintegrated gel particles then dominates and controls the discharge characteristics at high discharge rates.

Acknowledgements

This work was financially supported by the Swedish Research Council for National Sciences and by the Swedish Board for Technical Development. The ESCA instrument was bought from a grant by the Bank of Sweden Tercentenary Fund.

The visits to Lund by J. Jindra and by J. Mrha were part of an exchange programme between the Czechoslovak Academy of Sciences and the Swedish Academy of Engineering Sciences.

References

1 B. Klápště, J. Mrha, K. Micka, J. Jindra and V. Mareček, *J. Power Sources, 4* (1979) 349.
2 J. Mrha, I. Krejčí, Z. Zábranský, V. Koudelka and J. Malík, *J. Power Sources, 4* (1979) 239.
3 J. Jindra, J. Mrha, K. Micka, Z. Zábranský, B. Braunstein, J. Malík and V. Koudelka, in D. H. Collins (ed.), *Power Sources 6*, Academic Press, London, New York, San Francisco, 1977, p. 181.
4 K. Siegbahn, C. Nordling, A. Fahlman, R. Nordberg, K. Hamrin, J. Hedman, G. Johansson, T. Bergmark, S. E. Karlsson, I. Lindgren and B. Lindberg, *ESCA — Atomic, Molecular and Solid State Structure Studied by Means of Electron Spectroscopy*, Almquist and Wiksell, Uppsala, 1967.
5 J. Mrha, I. Krejčí, Z. Zábranský, V. Koudelka and J. Malík, *J. Power Sources, 4* (1979) 239.
6 V. Koudelka, J. Malík, J. Mrha, I. Krejčí and M. Špinka, *J. Power Sources, 6* (1981) 161.
7 G. Johansson, J. Hedman, A. Berndtsson, M. Klasson and B. Nilsson, *J. Electron. Spectrosc., 2* (1973) 295.
8 L. Y. Johansson, J. Mrha, M. Musilova and R. Larsson, *J. Power Sources, 2* (1977/78) 183.